Thermodynamics of Antiferromagnetic Solids in Magnetic Fields

Tomáš Brauner[a] and Christoph P. Hofmann[b]

[a] Department of Mathematics and Physics, University of Stavanger,
4036 Stavanger, Norway
[b] Facultad de Ciencias, Universidad de Colima
Colima C.P. 28045, Mexico

February 10, 2020

Abstract

We analyze the thermodynamic properties of antiferromagnetic solids subjected to a combination of mutually orthogonal uniform magnetic and staggered fields. Low-temperature series for the pressure, order parameter and magnetization up to two-loop order in the effective expansion are established. We evaluate the self-energy and the dispersion relation of the dressed magnons in order to discuss the impact of spin-wave interactions on thermodynamic observables.

1 Motivation

The literature on the thermodynamic properties of antiferromagnets in three spatial dimensions is considerable. Low-temperature representations for the free energy density, staggered magnetization, and other observables describing quantum Heisenberg antiferromagnets have been derived, e.g., in Refs. [1–10]. Various authors have furthermore discussed how an external magnetic field influences the low-temperature physics of antiferromagnets (see Refs. [11–21]).

Due to the complexity of the problem, approximations and ad hoc assumptions are usually made within the microscopic and phenomenological approaches that the above-mentioned articles are based upon. One particularly popular method to capture the low-energy physics of antiferromagnets is the spin-wave theory, based on the fact

that spin waves are the relevant low-energy degrees of freedom. The fact that these excitations are Goldstone bosons emerging due to the spontaneously broken internal symmetry $\mathrm{O}(3) \to \mathrm{O}(2)$, gives us, however, the opportunity to describe antiferromagnets in the systematic, model-independent language of effective field theory.

Originally, the effective Lagrangian method was developed for the spontaneously broken chiral symmetry in quantum chromodynamics that gives rise to the pions, kaons and the η-particle that constitute the corresponding Goldstone bosons: the lightest hadronic particles [22, 23]. The method, however, is universal and can be put to work whenever the phenomenon of spontaneous symmetry breaking takes place – it is perfectly suited to address condensed matter systems [24, 25], and amounts to a systematic low-energy (low-temperature) expansion of physical quantities.

Although antiferromagnets in three spatial dimensions have been analyzed with effective Lagrangians before [26–32], a systematic study of the manifestation of magnetic fields in the thermodynamic properties of the system is still lacking – both on the effective field theory and the conventional microscopic level. In particular, at the level where the spin-wave interaction becomes relevant in the thermodynamic observables, no references appear to be available. The present study hence closes a gap that has existed in the condensed-matter literature.

Recently, antiferromagnets subjected to magnetic fields were studied within the effective field theory framework, and their partition function was derived up to two loops, in both two [33] and three [34] spatial dimensions. In the present study, we build upon these previous works, but our focus is on separating genuine spin-wave interaction effects from the physics of a free gas of dressed magnons. This requires explicit evaluation of the magnon self-energy. Once having done so, we analyze the effect of magnon interactions on a number of physical observables: pressure, staggered magnetization (the order parameter) and magnetization.

Overall, the effect of the spin-wave interaction that enters at the two-loop level is very small compared to the dominant contribution due to the noninteracting Bose (magnon) gas. We observe that the spin-wave interaction in the pressure can be attractive or repulsive, depending on the specific location in parameter space determined by temperature, as well as magnetic and staggered field strength. If temperature is raised from $T = 0$ to a nonzero value T, while keeping magnetic and staggered field strengths fixed, the order parameter and the magnetization may decrease or increase as a consequence of the spin-wave interaction. Again, these subtle effects depend on temperature, as well as on the magnitude of the magnetic and staggered field.

The objective of our present study on antiferromagnetic solids parallels the situation regarding ferromagnetic solids. After Bloch had derived his famous $T^{3/2}$-law for the spontaneous magnetization [35], condensed matter physicists were struggling for decades with the important open theoretical question: what is the effect of the spin-wave interaction on the spontaneous magnetization of a three-dimensional fer-

romagnet, and how does the spin-wave interaction manifest itself in other thermodynamic observables of the system? This question has prompted more than a hundred references up to date and we believe that we are dealing here with a fundamental theoretical question also in the context of antiferromagnets.

Regarding ferromagnets, in a rather complicated monumental analysis [36, 37], Dyson gave the correct answer by showing that the spin-wave interaction first shows up in a correction term proportional to T^4 in the spontaneous magnetization. On the other hand, the same answer could be obtained by effective field theory methods in a much more transparent manner, and higher-order temperature powers in the spontaneous magnetization, and thermodynamic observables in general, could be derived straightforwardly [38, 39].

Here we address and answer the same fundamental open theoretical question for antiferromagnets subjected to a combination of mutually orthogonal uniform magnetic and staggered fields: what is the effect of the spin-wave interaction in the thermodynamic quantities like free energy density, pressure, order parameter and (uniform) magnetization? As we demonstrate, the systematic effective field theory gives a clearcut and simple answer.

It should be pointed out that the staggered field is not devoid of physical significance. In fact, as discussed in Ref. [40], the staggered field can be interpreted as an "effective" anisotropy field that mimics the magnetic anisotropy of the crystal and points into the direction of the "easy axis" of spontaneous staggered magnetization at $T = 0$. For a given antiferromagnetic sample the anisotropy field has a specific value that can in principle be determined by comparing our effective field theory predictions with experimental data.

The question is whether the extended Heisenberg model – i.e., the simple isotropic Heisenberg Hamiltonian with magnetic and staggered field terms incorporated – accurately describes a real antiferromagnetic solid. It is believed that some materials – like MnF_2 and $RbMnF_3$ – indeed are quite realistically captured by the extended Heisenberg model. Unfortunately, to the best of our knowledge, the available experimental data for these samples[1] cannot be directly compared to our findings which focus on the impact of the spin-wave interaction. As the present study reveals, spin-wave interaction effects in thermodynamic quantities are very small, such that it is extremely difficult – maybe impossible – to experimentally detect the manifestation of the spin-wave interaction in thermodynamic observables in a real antiferromagnetic sample.[2] Deviations from our predictions may also be attributed to effects we have not considered in our analysis: impurities, spin-orbit couplings, "interference" with other degrees of freedom like phonons, to name but just a few.

[1] For MnF_2 see, e.g., Refs. [41, 42], for $RbMnF_3$ see, e.g., Refs. [43, 44].

[2] The experimental situation regarding the detection of the spin-wave interaction in the thermodynamic properties of ferromagnets is not better.

Still, there exists another route to eventually test our effective field theory predictions: future numerical simulations of the "clean" three-dimensional antiferromagnetic Heisenberg model in presence of staggered and magnetic fields may be cross-checked against our findings and the validity of our predictions hence be rigorously confirmed.

The article is organized as follows. The two-loop representation for the free energy density is briefly reviewed in Sec. 2 to set the basis for the subsequent analysis. In Sec. 3, we then carry out the calculation of the one-loop magnon self-energies, and of the ensuing interaction part of the free energy density. (An alternative evaluation of the self-energies is given in appendix B.) Low-temperature series for the pressure, order parameter, and magnetization – in presence of magnetic and staggered fields – are derived in Sec. 4. In the same section the thermodynamic behavior of the system is discussed and illustrated using various figures. Emphasis is put on the impact of the spin-wave interaction at finite temperature. Finally, in Sec. 5 we conclude.

2 Free Energy Density: Two-Loop Representation

The paradigmatic microscopic description of antiferromagnets is based on the Heisenberg model, whose Hamiltonian in the simplest situation, where only the nearest neighbor spin interactions are taken into account, takes the form

$$\mathcal{H} = -J \sum_{n.n.} \vec{S}_m \cdot \vec{S}_n - \sum_n \vec{S}_n \cdot \vec{H} - \sum_n (-1)^n \vec{S}_n \cdot \vec{H}_s \,, \qquad J = const. \,, \tag{2.1}$$

where the summation in the first term extends over nearest neighbor spin pairs on a bipartite three-dimensional lattice. The exchange constant $J < 0$ defines the fundamental energy scale of the system. The first term is invariant under internal O(3) rotations, but the remaining terms that involve the magnetic field $\vec{H}$ and the staggered field $\vec{H}_s$, explicitly break the O(3) symmetry. Provided that these external fields are weak, the two terms represent small corrections, such that the O(3) symmetry is still approximate.

The effective field theory analysis of antiferromagnets is crucially based on the spontaneously broken approximate symmetry O(3) $\to$ O(2). It is important to keep in mind that the validity of the predictions of effective field theory is not limited to a specific microscopic model such as Eq. (2.1), but applies equally well to *any* microscopic system that possesses the same set of symmetries. For the reader's sake, we outline here briefly the basic setup of the effective field theory for antiferromagnets; more details can be found, for instance, in the pioneering work of Leutwyler [24] or in Ref. [34] whose notation we largely follow.

The starting point of the analysis is the effective Lagrangian (density) at the leading order of the low-energy, or derivative, expansion,

$$\mathcal{L}_{\text{eff}} = \frac{\rho_s}{2} D_\mu \vec{U} \cdot D^\mu \vec{U} + M_s \vec{H}_s \cdot \vec{U} \,, \tag{2.2}$$

where $\vec{U}$ is the effective spin variable, ρ_s represents the spin stiffness, $\vec{H}_s$ the staggered field, and M_s is the staggered magnetization at zero temperature and zero external fields. The covariant derivative $D_\mu \vec{U}$ incorporates the coupling of the spin degrees of freedom to an external magnetic field $\vec{H}$. Using Lorentz index notation, it reads

$$D_\mu \vec{U} = \partial_\mu \vec{U} + \delta_{\mu 0} \vec{H} \times \vec{U} \,. \tag{2.3}$$

In this paper, we focus on the special case where the magnetic field $\vec{H}$ and the staggered field $\vec{H}_s$ are mutually orthogonal. The coordinate frame can without loss of generality be chosen so that

$$\vec{H} = (0, H, 0) \,, \qquad \vec{H}_s = (H_s, 0, 0) \,. \tag{2.4}$$

The corresponding classical ground state of the antiferromagnet is found by maximizing the static, non-derivative part of the effective Lagrangian (2.2). It is easy to see that the direction of the staggered magnetization order parameter in the antiferromagnetic ground state then coincides with the direction of the staggered field, and is perpendicular to the direction of the magnetic field, $\langle \vec{U} \rangle = (1, 0, 0)$.

The subsequent evaluation of the partition function or any other observable is based on a parametrization of the unit vector $\vec{U}$ in terms of its fluctuations U^I, U^{II} around this ground state, which we choose as

$$\vec{U}(x) = (U^0(x), U^I(x), U^{II}(x)) \,, \qquad \text{where} \qquad U^0 = \sqrt{1 - (U^I)^2 - (U^{II})^2} \,. \tag{2.5}$$

The next step is to expand the effective Lagrangian (2.2) in powers of the fluctuation fields U^I, U^{II}. The leading, quadratic part of the Lagrangian gives the tree-level approximation to the dispersion relations of the two magnon modes,

$$\begin{aligned} \omega_I(\vec{k}) &= \sqrt{\vec{k}^2 + \frac{M_s H_s}{\rho_s} + H^2} \,, \\ \omega_{II}(\vec{k}) &= \sqrt{\vec{k}^2 + \frac{M_s H_s}{\rho_s}} \,. \end{aligned} \tag{2.6}$$

Note that only one of the magnons "senses" the magnetic field. Due to the relativistic nature of the dispersion relations, one can identify the magnon "masses" as

$$M_I^2 = \frac{M_s H_s}{\rho_s} + H^2 \,, \qquad M_{II}^2 = \frac{M_s H_s}{\rho_s} \,. \tag{2.7}$$

In the absence of external fields, the dispersion relations are identical: both are linear and ungapped, describing the two degenerate spin-wave branches.

The higher-order terms in the expansion of the effective Lagrangian in U^I, U^{II} represent bare interactions of magnons. With the corresponding Feynman rules, these

constitute the basic building blocks for a diagrammatical analysis of the thermodynamics of antiferromagnets using standard techniques of quantum field theory. Here we merely quote the main result of Ref. [34], the renormalized two-loop free energy density z of three-dimensional antiferromagnets in presence of the magnetic and staggered fields,

$$\begin{aligned}
z = z^{[0]} &- \tfrac{1}{2} g_0^I - \tfrac{1}{2} g_0^{II} \\
&- \frac{4H^2 + M_{II}^2}{8\rho_s} \big(g_1^I\big)^2 + \frac{M_{II}^2}{4\rho_s} g_1^I g_1^{II} - \frac{M_{II}^2}{8\rho_s} \big(g_1^{II}\big)^2 + \frac{2}{\rho_s}\, \hat{s}\, T^6 \\
&+ \frac{g_0^I}{32\pi^2\rho_s} \left[\frac{4H^2}{3} - 2\bar{e}_2 H^2 + M_{II}^2 - \frac{2M_{II}^4}{H^2} + 2H^2 \ln\frac{M_I^2}{\mu^2} + \frac{2M_{II}^6}{H^4} \ln\frac{M_I^2}{M_{II}^2} \right] \\
&+ \frac{g_0^{II}}{32\pi^2\rho_s} \left[(3 + \bar{e}_1 - 4\bar{e}_2) H^2 + 3H^2 \ln\frac{M_I^2}{\mu^2} \right] \\
&+ \frac{g_1^I}{32\pi^2\rho_s} \left[\frac{H^4}{3} + \left(-\frac{1}{6} + \frac{\bar{e}_1}{3} - \frac{4\bar{e}_2}{3} + \frac{\bar{k}_1}{2} \right) H^2 M_{II}^2 + (-2 - \bar{k}_1 + \bar{k}_2)\, M_{II}^4 \right. \\
&\qquad \left. - \frac{2M_{II}^6}{H^2} + \frac{H^2 M_{II}^2}{2} \ln\frac{M_I^2}{\mu^2} + \left(\frac{3M_{II}^4}{2} + \frac{3M_{II}^6}{H^2} + \frac{2M_{II}^8}{H^4} \right) \ln\frac{M_I^2}{M_{II}^2} \right] \\
&+ \frac{g_1^{II}}{32\pi^2\rho_s} \left[\left(2 + \bar{e}_1 - 4\bar{e}_2 + \frac{\bar{k}_1}{2} \right) H^2 M_{II}^2 + (\bar{k}_2 - \bar{k}_1) M_{II}^4 \right. \\
&\qquad \left. + \frac{5H^2 M_{II}^2}{2} \ln\frac{M_I^2}{\mu^2} + \frac{M_{II}^4}{2} \ln\frac{M_I^2}{M_{II}^2} \right] . \qquad (2.8)
\end{aligned}$$

The various quantities appearing therein are defined as follows. The kinematical functions g_r^I and g_r^{II} describe the free Bose (magnon) gas and read

$$\begin{aligned}
g_r^{I,II}(H_s, H, T) &= 2 \int_0^\infty \frac{\mathrm{d}\rho}{(4\pi)^2}\, \rho^{r-3} \exp(-\rho M_{I,II}^2) \sum_{n=1}^\infty \exp(-n^2/4\rho T^2) \qquad (2.9) \\
&= \frac{1}{(4\pi)^2} \frac{4\sqrt{\pi} T^{4-2r}}{\Gamma\left(\frac{5}{2} - r\right)} \int_0^\infty \mathrm{d}x \frac{x^{4-2r}}{\sqrt{x^2 + (M_{I,II}/T)^2}} \frac{1}{e^{\sqrt{x^2 + (M_{I,II}/T)^2}} - 1} .
\end{aligned}$$

Then, the dimensionless function $\hat{s}$ incorporates the nontrivial part of the free energy density: the part that cannot be reduced to products of kinematical functions g_r^I and g_r^{II}. It is defined by a set of lengthy expressions that will not be needed in the following. In order not to interrupt the flow of argument, the precise definition is therefore relegated to Appendix A. Likewise, the zero-temperature part of the free energy density, $z^{[0]}$, is of no concern to the present paper, and is thus only spelled out explicitly in Appendix A.

In Fig. 1, we provide a 3D-plot of $\hat{s}$. Note that the function $\hat{s}$, much like the kinematical functions $g_r^{I,II}$, can be expressed in terms of the dimensionless parameters σ_H and σ,

$$\sigma_H = \frac{H}{2\pi T} , \qquad \sigma = \frac{\sqrt{M_s H_s}}{2\pi\sqrt{\rho_s} T} . \qquad (2.10)$$

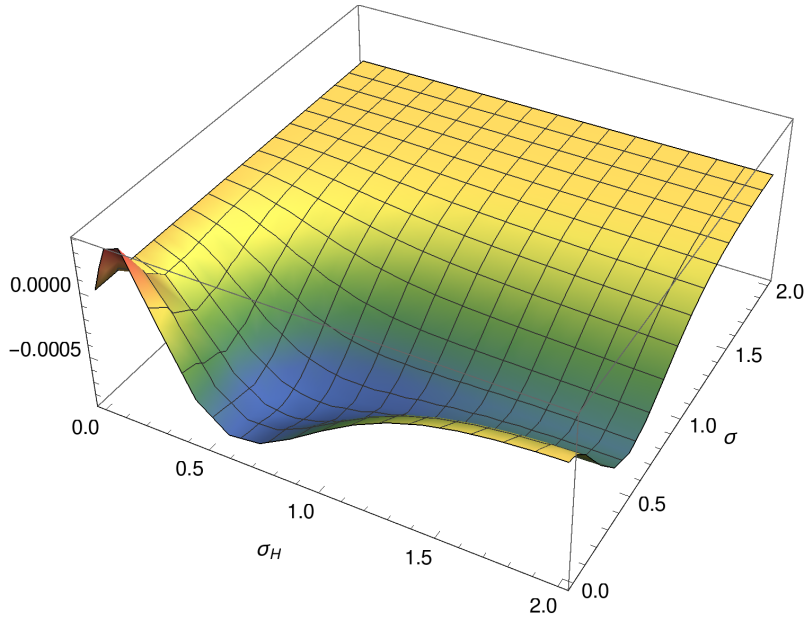

Figure 1: [Color online] 3D-plot of the function $\hat{s}(\sigma, \sigma_H)$, in terms of the dimensionless parameters $\sigma_H = H/(2\pi T)$ and $\sigma = \sqrt{M_s H_s}/(2\pi\sqrt{\rho_s} T)$.

These parameters measure the strength of the magnetic and the staggered fields with respect to the temperature.

Finally, the quantities $\overline{e}_1, \overline{e}_2, \overline{k}_1, \overline{k}_2$ are the so-called renormalized next-to-leading-order (NLO) effective constants. These are pure numbers of order unity,

$$\overline{e}_1, \overline{e}_2, \overline{k}_1, \overline{k}_2 \;\approx\; 1\,, \tag{2.11}$$

whose actual values depend on the chosen renormalization scale μ via the renormalization group equations

$$\overline{e}_i(\mu_2) = \overline{e}_i(\mu_1) + \ln\frac{\mu_1^2}{\mu_2^2}\,, \qquad \overline{k}_i(\mu_2) = \overline{k}_i(\mu_1) + \ln\frac{\mu_1^2}{\mu_2^2}\,. \tag{2.12}$$

It should be pointed out that the μ-dependence of the NLO effective constants is canceled by the μ-dependent logarithms in Eq. (2.8): indeed, the free energy density, and all thermodynamic observables derived from there, does not depend on the renormalization scale.

3 Dressed Magnons and Interaction Free Energy Density

Naively, one might expect that the first line of our result (2.8) for the free energy density, that is its one-loop part, corresponds to a gas of free magnons, while all the rest captures magnon–magnon interactions. That would, however, be premature: the magnons get dressed by self-energy corrections even at $T = 0$. Part of the thermal two-loop free energy density can then be accounted for as the free energy density of such dressed, yet noninteracting, magnons. Whatever is left can be considered as a genuine interaction effect.

Such a splitting of the two-loop contributions to the free energy density into free and interaction parts makes sense not only physically, but also mathematically. It will namely turn out that the interaction part of the two-loop free energy density is independent altogether of the NLO effective constants $\overline{e}_1, \overline{e}_2, \overline{k}_1, \overline{k}_2$. By the same token, this interaction free energy density is explicitly independent of the renormalization scale μ. It is, in fact, determined solely by the leading-order effective Lagrangian (2.2) that involves the spin stiffness ρ_s as the only low-energy effective coupling: the question, e.g., of whether the spin-wave interaction in the pressure is attractive or repulsive, can hence be answered rigorously in a model-independent and parameter-free manner.

To see what needs to be done, consider a quasiparticle which, just like our magnons, has a relativistic dispersion relation with mass M, $\omega = \sqrt{\vec{k}^2 + M^2}$. The complete inverse propagator for such a quasiparticle in imaginary time will take the form

$$\mathcal{D}(k_0, \vec{k}) = k_0^2 + \vec{k}^2 + M^2 + \Pi(k_0, \vec{k})\,, \tag{3.1}$$

where $\Pi(k_0, \vec{k})$ is the self-energy due to quantum corrections. The exact dispersion relation of the quasiparticle is determined by the position of the pole in $\mathcal{D}$ as a function of frequency k_0. In case a mere expansion up to certain fixed order is desired, we can solve for the pole iteratively. It is then easy to see that the NLO (one-loop) self-energy Π_{NLO} gives rise to the following "dressed" dispersion relation,

$$\omega(\vec{k}) = \sqrt{\vec{k}^2 + M^2 + \epsilon(\vec{k})}\,, \qquad \epsilon(\vec{k}) = \Pi_{NLO}(k_0, \vec{k})\Big|_{k_0 \to -i\sqrt{\vec{k}^2+M^2}}\,. \tag{3.2}$$

The free energy density of the noninteracting dressed magnons can now be obtained from the basic formula

$$z_{free} = z_{free}^{[0]} + T \int \frac{\mathrm{d}^3 k}{(2\pi)^3}\, \ln\left[1 - e^{-\omega(\vec{k})/T}\right]\,. \tag{3.3}$$

Here $z_{free}^{[0]}$ is the (temperature-independent) vacuum free energy density. The leading-order dispersion relation, $\omega(\vec{k}) = \sqrt{\vec{k}^2 + M^2}$, gives the dominant contribution to the

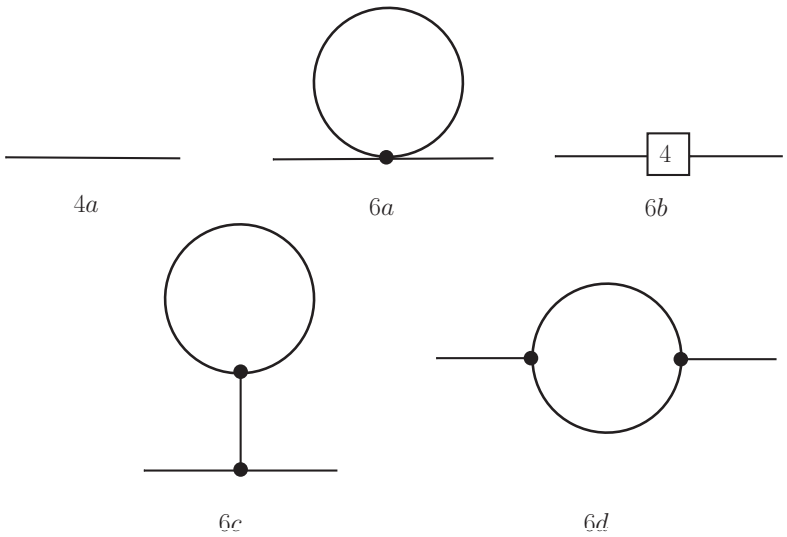

Figure 2: Feynman graphs for the magnon self-energies in the $d = 3 + 1$ antiferromagnet up to one-loop order. Filled circles represent vertices from the leading-order effective Lagrangian $\mathcal{L}^2_{eff}$, the box with the number 4 corresponds to a vertex from the NLO Lagrangian $\mathcal{L}^4_{eff}$. Loops are suppressed by two powers of momentum.

thermal part of the free energy density, $-\frac{1}{2}g_0(M)$, where the kinematical function g_0 is defined in Eq. (2.9). Let us finally expand the function $\epsilon(\vec{k})$ as[3]

$$\epsilon(\vec{k}) = \epsilon_0 + \epsilon_1 \vec{k}^2 \,. \tag{3.4}$$

Expanding likewise Eq. (3.3) to first order in $\epsilon(\vec{k})$ then implies that the thermal part of the free energy density of dressed magnons to NLO is

$$z^T_{free} = -\frac{1}{2}g_0(M) + \frac{1}{2}\epsilon_0 g_1(M) + \frac{3}{4}\epsilon_1 g_0(M) \,. \tag{3.5}$$

This will be our master formula. All that is left to do is to evaluate the $T = 0$ self-energies of the magnons on their "mass shell", that is at $k_0^2 = -(\vec{k}^2 + M^2)$.

The generic topologies of Feynman diagrams that contribute to the one-loop self-energy are shown in Fig. 2. The calculation itself is a matter of a simple exercise in graduate-level quantum field theory, and we therefore only quote the main results. The one-loop (imaginary-time) self-energies of the two magnons are given by

$$\begin{aligned} -\rho_s \Pi_I(k) = &\left(M_I^2 - k^2 - 4H^2 - \frac{3M_s H_s}{2\rho_s} \right) I_0(M_I) - \frac{M_s H_s}{2\rho_s} I_0(M_{II}) \\ &+ \frac{H^2}{4\pi^2 \varepsilon} \left(\frac{\vec{k}^2}{3} - \frac{k^2}{4} - \frac{M_s H_s}{2\rho_s} - \frac{3H^2}{4} \right) \end{aligned}$$

[3]Dependence only on $\vec{k}^2$ follows from rotational invariance. It will be shown below that at NLO, there are no higher-order terms in the expansion in $\vec{k}^2$.

$$
\begin{aligned}
&+\frac{H^2}{4\pi^2}\int_0^1 \mathrm{d}x\bigg[-\frac{\tilde{M}^2}{2}+\left(M_{II}^2+\vec{k}^2x^2-\frac{3\tilde{M}^2}{2}\right)\left(-\gamma_E+\ln\frac{4\pi\mu^2}{\tilde{M}^2}\right)\bigg]\\
&+(a_Ik_0^2+b_I\vec{k}^2+c_I)\,, \qquad (3.6)\\
-\rho_s\Pi_{II}(k)=&\left(M_{II}^2-k^2-\frac{3M_sH_s}{2\rho_s}\right)I_0(M_{II})-\frac{M_sH_s}{2\rho_s}I_0(M_I)-\frac{H^2k_0^2}{8\pi^2\varepsilon}\\
&-\frac{H^2k_0^2}{8\pi^2}\int_0^1\mathrm{d}x\left[-\gamma_E+\ln\frac{4\pi\mu^2}{M_I^2+k^2x(1-x)}\right]+(a_{II}k_0^2+b_{II}\vec{k}^2+c_{II})\,,
\end{aligned}
$$

where x is a Feynman parameter, $\varepsilon=2-d/2$ is the expansion parameter of dimensional regularization,

$$
\tilde{M}^2=k^2x(1-x)+\frac{M_sH_s}{\rho_s}+H^2x\,, \qquad (3.7)
$$

and we denoted the frequency and momentum collectively as k so that $k^2=k_0^2+\vec{k}^2$. Moreover, I_0 is a zero-temperature momentum integral defined by

$$
I_0(M)=\mu^{2\varepsilon}\int\frac{\mathrm{d}^dp}{(2\pi)^d}\frac{1}{p^2+M^2}\,. \qquad (3.8)
$$

Finally, $a_{I,II}$, $b_{I,II}$, $c_{I,II}$ are counterterms whose values were fixed in Ref. [34] by the calculation of the two-loop free energy. They are given by

$$
\begin{aligned}
a_I&=-2\left(2e_1H^2+2e_2H^2+\frac{k_1M_sH_s}{\rho_s}\right),\\
a_{II}&=-2\left(6e_1H^2+6e_2H^2+\frac{k_1M_sH_s}{\rho_s}\right),\\
b_I&=-2\left(2e_1H^2+\frac{k_1M_sH_s}{\rho_s}\right),\\
b_{II}&=-2\left(2e_1H^2+2e_2H^2+\frac{k_1M_sH_s}{\rho_s}\right),\\
c_I&=-2\left(2e_1H^4+2e_2H^4+\frac{3k_1H^2M_sH_s}{2\rho_s}+\frac{k_2M_s^2H_s^2}{\rho_s^2}\right),\\
c_{II}&=-2\left(\frac{k_1H^2M_sH_s}{2\rho_s}+\frac{k_2M_s^2H_s^2}{\rho_s^2}\right),
\end{aligned} \qquad (3.9)
$$

where

$$
e_{1,2}=\gamma_{1,2}\left(\lambda+\frac{\bar{e}_{1,2}}{32\pi^2}\right), \qquad k_{1,2}=\gamma_{3,4}\left(\lambda+\frac{\bar{k}_{1,2}}{32\pi^2}\right). \qquad (3.10)
$$

The numerical coefficients γ_i are fixed by $\gamma_1=-\frac{1}{6}$, $\gamma_2=\frac{2}{3}$, $\gamma_3=\gamma_4=1$. Finally, λ is a basic divergence that appears in the loop integrals. In dimensional regularization, it acquires the form

$$
\lambda=\frac{\Gamma(-1+\varepsilon)}{2(4\pi)^{2-\varepsilon}}=-\frac{1}{32\pi^2}\left[\frac{1}{\varepsilon}+1-\gamma_{\mathrm{E}}+\ln 4\pi+\mathcal{O}(\varepsilon)\right], \qquad (3.11)
$$

where $\gamma_{\rm E} \approx 0.577$ is the Euler–Mascheroni constant.

In the next step, we put the self-energies on the mass shell by replacing $k_0^2 \to -(\vec{k}^2 + M_{I,II}^2)$. It also proves convenient to extract the explicit dependence of the integral over the Feynman parameter on the renormalization scale. Making use of the auxiliary functions

$$\begin{aligned}
\mathcal{K}_1(a,b) &= -\int_0^1 \mathrm{d}x \ln\left[a^2 - b^2 x(1-x)\right], \\
\mathcal{K}_2(a,b) &= \frac{1}{2}\int_0^1 \mathrm{d}x \left\{\left[3a^2x^2 + b^2(1-3x)\right]\ln\left[a^2x^2 + b^2(1-x)\right] - \left[a^2x^2 + b^2(1-x)\right]\right\}, \\
\mathcal{K}_3(a,b) &= -\int_0^1 \mathrm{d}x\, x^2 \ln\left[a^2x^2 + b^2(1-x)\right],
\end{aligned} \tag{3.12}$$

the on-shell self-energies can be rewritten as

$$\begin{aligned}
-\rho_s \Pi_I(\vec{k}) = {} & \frac{M_s H_s}{2\rho_s}[I_0(M_I) - I_0(M_{II})] - 2H^2 I_0(M_I) \\
& + \frac{H^2}{4\pi^2}\left(\frac{\vec{k}^2}{3} - \frac{M_s H_s}{4\rho_s} - \frac{H^2}{2}\right)\left(\frac{1}{\varepsilon} - \gamma_E + \ln\frac{4\pi\mu^2}{T^2}\right) \\
& + \frac{H^2 T^2}{4\pi^2}\left[\mathcal{K}_2(M_I/T, M_{II}/T) + \frac{\vec{k}^2}{T^2}\mathcal{K}_3(M_I/T, M_{II}/T)\right] \\
& + (a_I k_0^2 + b_I \vec{k}^2 + c_I), \\
-\rho_s \Pi_{II}(\vec{k}) = {} & \frac{M_s H_s}{2\rho_s}[I_0(M_{II}) - I_0(M_I)] \\
& + \frac{H^2}{8\pi^2}(\vec{k}^2 + M_{II}^2)\left[\frac{1}{\varepsilon} - \gamma_E + \ln\frac{4\pi\mu^2}{T^2} + \mathcal{K}_1(M_I/T, M_{II}/T)\right] \\
& + (a_{II} k_0^2 + b_{II}\vec{k}^2 + c_{II}).
\end{aligned} \tag{3.13}$$

Note that these are linear functions of $\vec{k}^2$, as anticipated in Eq. (3.4). Using these expressions together with Eq. (3.5) yields the thermal free energy density of non-interacting dressed magnons. Once subtracted from the full two-loop free energy density (2.8), this gives the part of free energy density due to spin wave interaction,

$$z_{int} = \frac{H^2}{2\rho_s}(g_1^I)^2 - \frac{M_s H_s}{8\rho_s^2}(g_1^I - g_1^{II})^2 - \frac{H^2}{\rho_s}\mathcal{X}_2 + z^{[0]} - z^{[0]}_{free}, \tag{3.14}$$

where the two-loop thermal integral $\mathcal{X}_2$ is defined by [34]

$$\begin{aligned}
\mathcal{X}_2 = \int \frac{\mathrm{d}^3\vec{p}}{(2\pi)^3}\frac{\mathrm{d}^3\vec{q}}{(2\pi)^3}\frac{\vec{k}^2 + M^2}{4\omega_p^I \omega_q^I \omega_k^{II}}\Bigg[& n(\omega_p^I) n(\omega_q^I)\left(\frac{1}{\omega_k^{II} + \omega_p^I + \omega_q^I} + \frac{1}{\omega_k^{II} - \omega_p^I + \omega_q^I}\right. \\
& \left. + \frac{1}{\omega_k^{II} + \omega_p^I - \omega_q^I} + \frac{1}{\omega_k^{II} - \omega_p^I - \omega_q^I}\right) + 2n(\omega_k^{II}) n(\omega_p^I)\left(\frac{1}{\omega_k^{II} + \omega_p^I + \omega_q^I}\right.
\end{aligned}$$

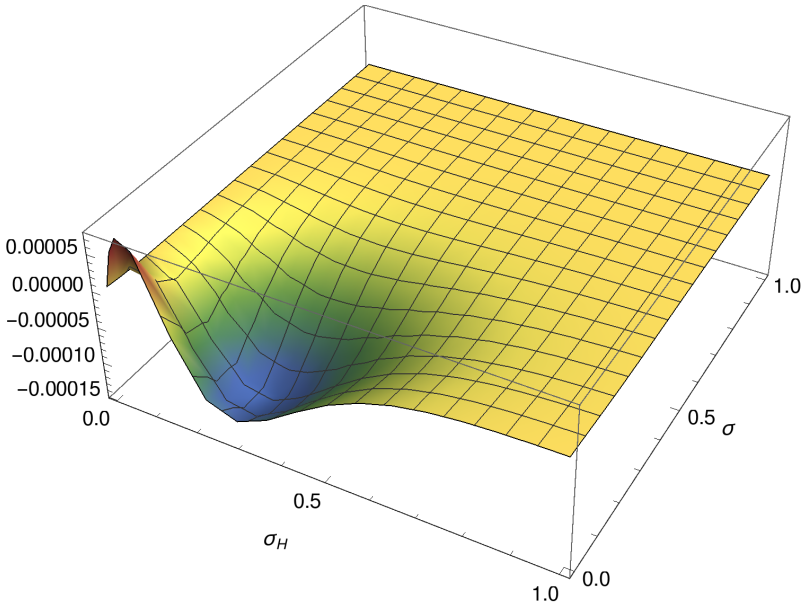

Figure 3: [Color online] 3D-plot of the function $\hat{\mathcal{X}}_2(\sigma, \sigma_H)$, in terms of the dimensionless parameters $\sigma_H = H/(2\pi T)$ and $\sigma = \sqrt{M_s H_s}/(2\pi\sqrt{\rho_s} T)$.

$$+ \frac{1}{\omega_k^{II} - \omega_p^I + \omega_q^I} + \frac{1}{-\omega_k^{II} + \omega_p^I + \omega_q^I} + \frac{1}{-\omega_k^{II} - \omega_p^I + \omega_q^I} \Bigg) \Bigg] , \tag{3.15}$$

where $\vec{k} = -(\vec{p} + \vec{q})$ and we have for the sake of brevity used the shorthand notation

$$\omega_p^{I,II} = \sqrt{\vec{p}^2 + M_{I,II}^2} , \qquad n(x) = \frac{1}{e^{x/T} - 1} . \tag{3.16}$$

In analogy to the sunset function $\hat{s}$, in Fig. 3 we provide a 3D-plot of the normalized two-loop thermal integral $\hat{\mathcal{X}}_2$ defined by

$$2\hat{\mathcal{X}}_2 = \frac{\rho_s}{T^6} \left(- \frac{H^2}{\rho_s} \mathcal{X}_2 \right) . \tag{3.17}$$

Eq. (3.14) is our main result, on which the following discussion of interaction effects in various physical observables is largely based. While Eq. (3.14) has been obtained within the momentum-space approach, in Appendix B we derive an alternative representation for the two-loop free energy density using coordinate-space techniques.

4 Low-Temperature Series

The effective field theory expansion of the free energy density, Eq. (2.8), is valid at low temperatures and in weak external fields. More precisely, the quantities T, H, H_s have

to be small compared to a characteristic scale inherent in the underlying microscopic system. In the present case of the Heisenberg antiferromagnet, the thermal scale is given by the Néel temperature T_N. The actual definition of *low* temperature and *weak* field is somewhat arbitrary. To be concrete, here we choose

$$T,\, H,\, M_{II}(\propto \sqrt{H_s}) \;\lesssim 0.4\; T_N\,. \tag{4.1}$$

The question then is how T_N is related to the exchange integral J that defines the non-thermal microscopic scale in the Heisenberg Hamiltonian (2.1). To that end we utilize the one-loop effective result, Eq. (4.12), for the order parameter M_s as a function of temperature in the absence of external fields,

$$M_s(T) = M_s\left(1 - \frac{1}{12\rho_s}T^2\right)\,. \tag{4.2}$$

Setting $M_s(T) = 0$, we obtain an approximate connection between T_N and the spin stiffness,

$$T_N \;\approx\; 3.5\,\sqrt{\rho_s}\,. \tag{4.3}$$

According to Ref. [28], for the simple cubic $S = \frac{1}{2}$ antiferromagnet that we choose as a representative system, we have[4]

$$\rho_s \approx 0.37\,|J|^2\,, \tag{4.4}$$

such that

$$T,\, H,\, M_{II}(\propto \sqrt{H_s}) \;\lesssim 0.4\; T_N \approx 1.4\,\sqrt{\rho_s} \approx\; |J|\,. \tag{4.5}$$

To depict the low-energy behavior of the system, it is convenient to choose the dimensionless parameters t, m_H, m,

$$t \equiv \frac{T}{\sqrt{\rho_s}}\,, \qquad m_H \equiv \frac{H}{\sqrt{\rho_s}}\,, \qquad m \equiv \frac{\sqrt{M_s H_s}}{\rho_s}\,. \tag{4.6}$$

These ratios are then all to be smaller than one for the effective theory to be valid, and measure the temperature and field strength with respect to the microscopic scale J. Of course, the actual value of J depends on the specific antiferromagnetic sample. Typically, the order of magnitude of J is in the meV-range (see, e.g., Ref. [45]).

4.1 Pressure

If the system is homogeneous, the temperature-dependent piece in the free energy density determines the pressure,

$$P = z^{[0]} - z\,, \tag{4.7}$$

[4]The square of the leading-order effective coupling constant F, used in Ref. [28], corresponds to the spin stiffness: $\rho_s = F^2$ (see Ref. [26]).

where $z^{[0]}$ is the vacuum energy density. The structure of the low-temperature expansion becomes explicit by rewriting the kinematical functions g_r in terms of the dimensionless functions h_r as

$$g_0(m, m_H, t) = T^4\, h_0(m, m_H, t), \quad g_1(m, m_H, t) = T^2\, h_1(m, m_H, t)\,, \tag{4.8}$$

with the result

$$\begin{aligned} P(T, H_s, H) &= \hat{p}_1\, T^4 + \hat{p}_2\, T^6 + \mathcal{O}(T^8)\,, \\ \hat{p}_1(T, H_s, H) &= \tfrac{1}{2}(h_0^I + h_0^{II})\,. \end{aligned} \tag{4.9}$$

We refrain from listing the lengthy expression for the coefficient $\hat{p}_2$: up to an overall minus sign, it corresponds to lines 2–8 in the representation for the free energy density, Eq. (2.8). The dominant contribution (order T^4) refers to the free Bose gas, while the spin-wave interaction sets in at the T^6-level.

However, not all T^6-contributions in $\hat{p}_2$ are related to the spin-wave interaction, as explained in the previous section. The interaction part of the free energy density is given by Eq. (3.14). To explore the impact of the interaction on pressure, we define the dimensionless ratio

$$\xi_P(T, H_s, H) = \frac{P_{int}(T, H_s, H)}{P_{Bose}(T, H_s, H)} = \frac{\hat{p}_2^{int}\, T^6}{\hat{p}_1 T^4}\,, \tag{4.10}$$

that captures the sign and strength of the spin-wave interaction with respect to the leading free magnon gas contribution. The coefficient $\hat{p}_2^{int}$ refers to the purely interaction part, given by Eq. (3.14).

In Fig. 4 we show ξ_P for four values of temperature $t = \{0.02, 0.05, 0.10, 0.30\}$. The plots illustrate that the effect of the interaction – compared to the free magnon gas contribution – is very small. At lower temperatures, the spin-wave interaction may be attractive or repulsive in the parameter domain we consider, depending on the actual values of the magnetic and staggered field. While at lower temperatures the repulsive region dominates, at more elevated temperatures, as Fig. 4 suggests, the interaction becomes purely attractive. Note that, in the absence of the magnetic field, there is no interaction contribution at two-loop order, in agreement with earlier studies [28].

4.2 Order Parameter

The staggered magnetization (order parameter) is given by the derivative of the free energy density with respect to the staggered field,

$$M_s(T, H_s, H) = -\frac{\partial z(T, H_s, H)}{\partial H_s}\,. \tag{4.11}$$

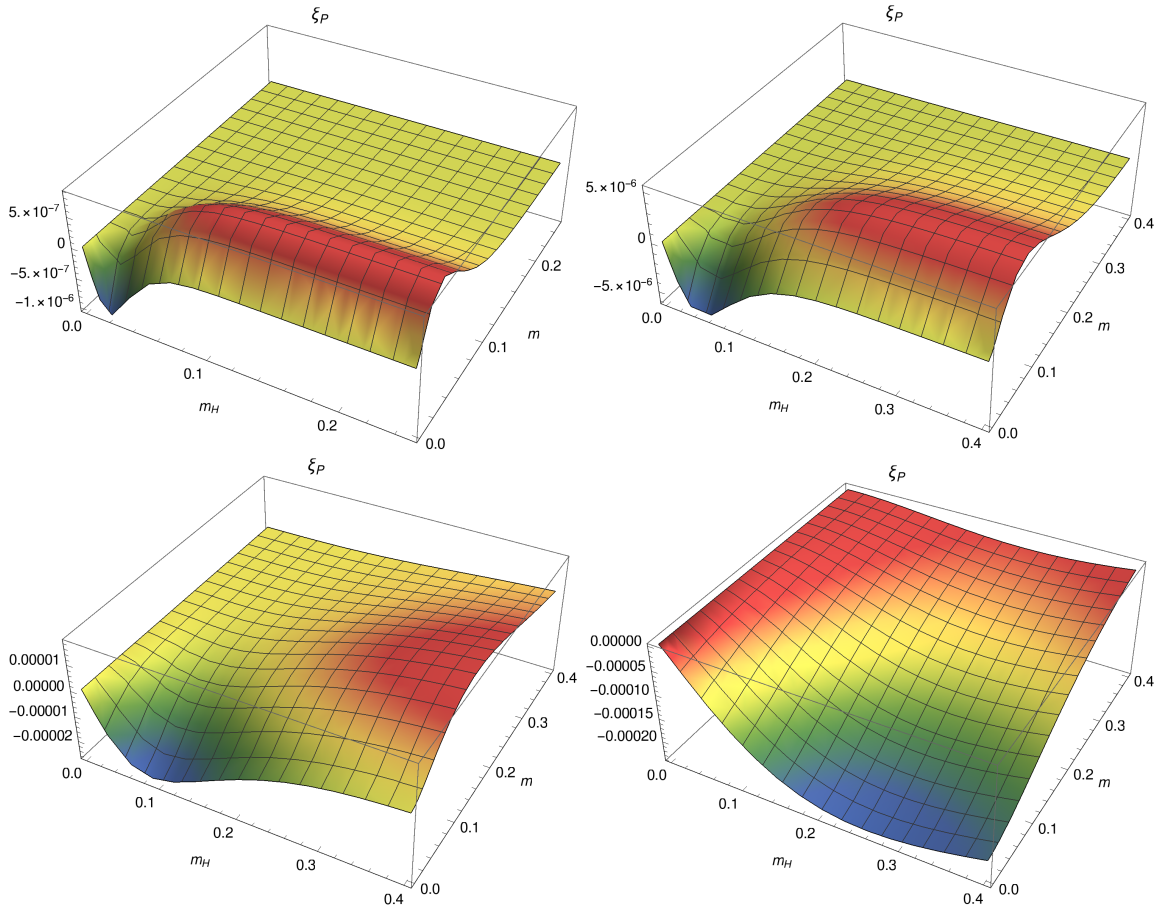

Figure 4: [Color online] Impact of the spin-wave interaction on pressure – quantified by $\xi_P(T, H_s, H)$ – of $d = 3 + 1$ antiferromagnets subjected to magnetic and staggered fields. The temperatures are $t = \{0.02, 0.05, 0.10, 0.30\}$ (top left to bottom right).

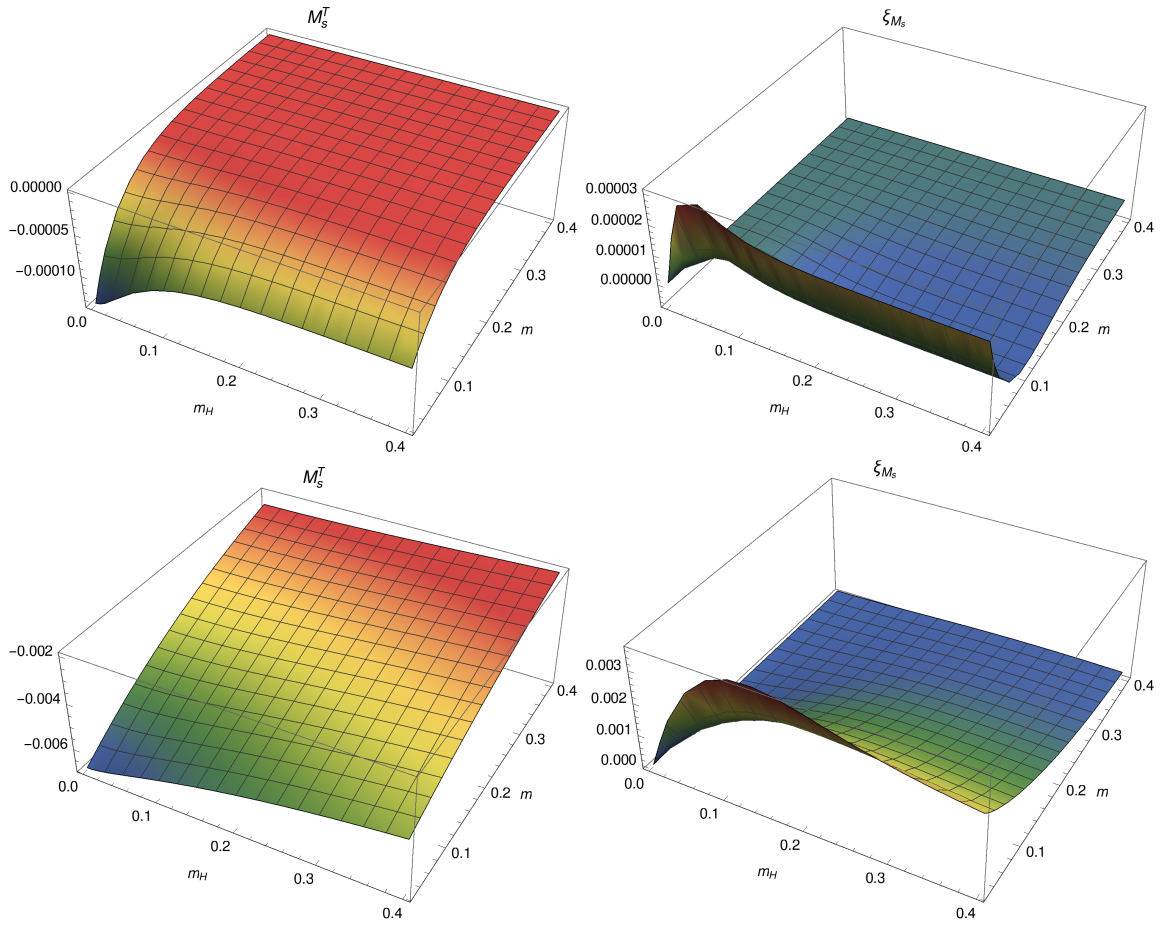

Figure 5: [Color online] Antiferromagnets subjected to mutually orthogonal staggered and magnetic fields at the temperatures $t = 0.05$ (upper panel) and $t = 0.30$ (lower panel). Left: Full temperature-dependent part of the staggered magnetization $M_s^T(T, H_s, H)$. Right: Impact of the genuine spin-wave interaction on the staggered magnetization – quantified by $\xi_{M_s}(T, H_s, H)$.

Its low-temperature expansion amounts to

$$\begin{aligned} M_s(T, H_s, H) &= M_s(0, H_s, H) + \hat{m}_1 T^2 + \hat{m}_2 T^4 + \mathcal{O}(T^6)\,, \\ \hat{m}_1(T, H_s, H) &= -\frac{M_s}{2\rho_s}\left(h_1^I + h_1^{II}\right), \end{aligned} \tag{4.12}$$

where the spin-wave interaction enters at the next-to-leading order (T^4). The zero-temperature staggered magnetization $M_s(0, H_s, H)$ involves interaction as well as non-interaction pieces.

It is again convenient to measure the effect of spin-wave interactions by a dimen-

sionless ratio,

$$\xi_{M_s}(T, H_s, H) = \frac{M_{s,int}(T, H_s, H)}{|M_{s,Bose}(T, H_s, H)|} = \frac{\hat{m}_2^{int}\, T^4}{|\hat{m}_1| T^2}\,, \tag{4.13}$$

defined relative to the free Bose gas contribution. In Fig. 5 we provide plots of $\xi_{M_s}(T, H_s, H)$ for the temperatures $t = \{0.05, 0.30\}$. In addition, for the same two temperatures, we depict the full temperature-dependent staggered magnetization,

$$M_s^T(T, H_s, H) = \hat{m}_1 T^2 + \hat{m}_2\, T^4\,. \tag{4.14}$$

As one expects, the quantity $M_s^T(T, H_s, H)$ is negative: the value of the order parameter drops when temperature is raised from $T = 0$ to a nonzero value T – while keeping H_s and H fixed. Interestingly, the ratio $\xi_{M_s}(T, H_s, H)$ is mainly positive in the entire parameter region $m_H, m \leq 0.4$. In a plain language, this implies that if temperature is raised from $T = 0$ to a nonzero value T – while keeping H_s and H fixed – the value of the staggered magnetization increases on account of the spin-wave interaction.

4.3 Magnetization

The magnetization is given by the derivative of the free energy density with respect to the magnetic field,

$$M(T, H_s, H) = -\frac{\partial z(T, H_s, H)}{\partial H}\,. \tag{4.15}$$

The low-temperature expansion takes the form

$$\begin{aligned} M(T, H_s, H) &= M(0, H_s, H) + \tilde{m}_1 T^2 + \tilde{m}_2 T^4 + \mathcal{O}(T^6)\,, \\ \tilde{m}_1(T, H_s, H) &= -H h_1^I\,. \end{aligned} \tag{4.16}$$

As for the order parameter M_s, the spin-wave interaction in the magnetization sets in at order T^4.

In Fig. 6, on the left-hand sides, we show the full temperature-dependent magnetization,

$$M_T(T, H_s, H) = \frac{\tilde{m}_1 T^2 + \tilde{m}_2\, T^4}{\rho_s^{3/2}}\,, \tag{4.17}$$

for the temperatures $t = \{0.05, 0.30\}$.[5] As one would expect, M_T takes negative values in the whole parameter region we depict: when the magnetic and staggered field strengths are kept fixed, the magnetization drops as temperature increases from $T = 0$ to nonzero T.

Remarkably, as illustrated on the right-hand sides of Fig. 6, the sign of the quantity

$$M_T^{int}(T, H_s, H) = \frac{\tilde{m}_2^{int}\, T^4}{\rho_s^{3/2}}\,, \tag{4.18}$$

[5]Normalization by $\rho_s^{3/2}$ guarantees that $M_T(T, H_s, H)$ is dimensionless.

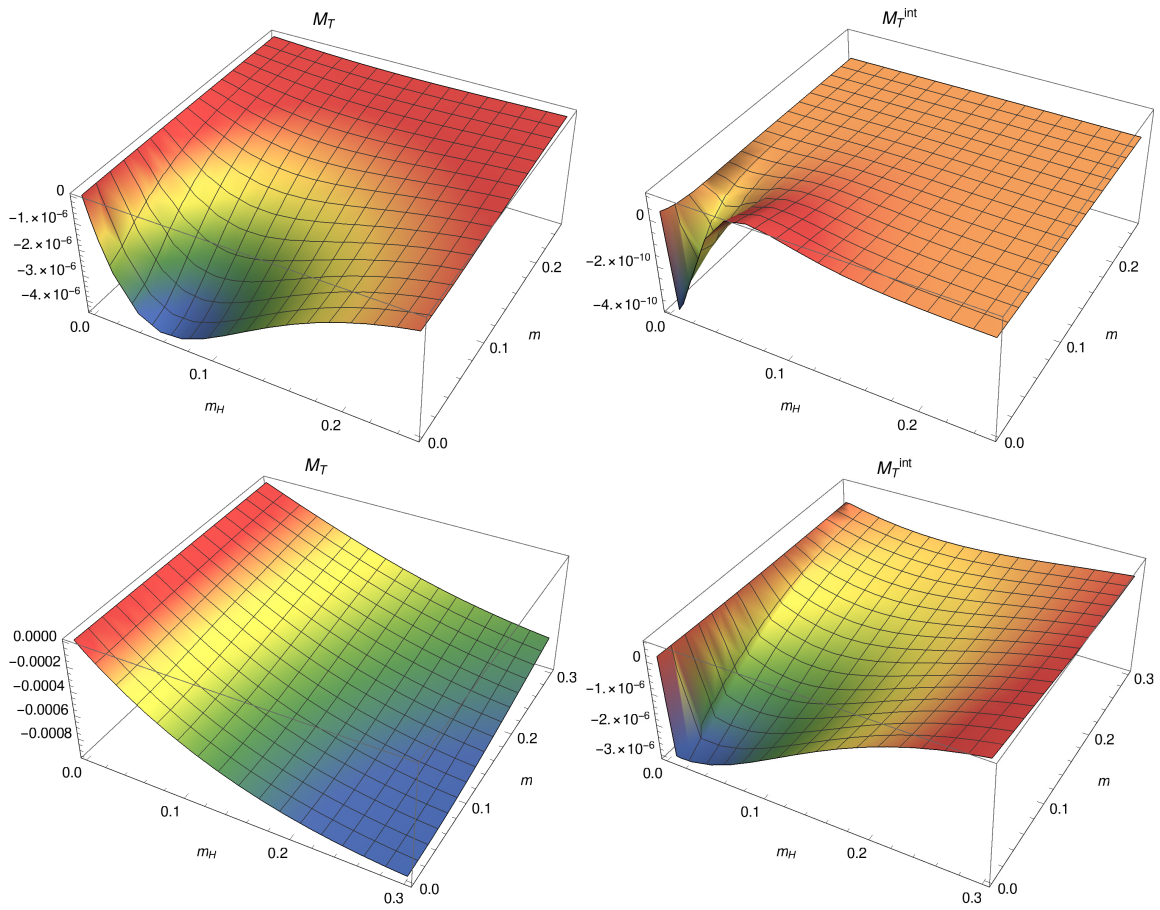

Figure 6: [Color online] Antiferromagnets subjected to mutually orthogonal staggered and magnetic fields at the temperatures $t = 0.05$ (upper panel) and $t = 0.30$ (lower panel). Left: Full temperature-dependent part of the magnetization $M_T(T, H_s, H)$. Right: Impact of the genuine spin-wave interaction on the magnetization – quantified by $M_T^{int}(T, H_s, H)$.

that only measures the effect of the spin-wave interaction, may take positive values. This indicates that if temperature is raised from $T = 0$ to a nonzero value T – while keeping H_s and H fixed – the value of the magnetization increases as a consequence of the spin-wave interaction. But it should be emphasized that these effects are rather subtle: the spin-wave interaction – measured by $M_T^{int}(T, H_s, H)$ – is very weak.

5 Conclusions

Antiferromagnets subjected to magnetic and staggered fields can be addressed straightforwardly with the systematic effective Lagrangian method. Starting from the two-loop representation of the partition function, we have discussed the low-temperature behavior of $d = 3 + 1$ antiferromagnets in a configuration of mutually orthogonal external magnetic and staggered fields.

To have a clear picture of what "interaction" means in the free energy density – and any other thermodynamic quantity derived from there – we have evaluated the self-energy of the two magnons up to one-loop order. This then allowed us to extract their dispersion relations and to rewrite the free energy density in terms of the dressed magnons. In particular, all next-to-leading-order low-energy constants (whose values are a priori unknown) can be absorbed into the dispersion relations of the dressed magnons. The remaining terms at the two-loop order then correspond to the spin-wave interaction which is fully fixed by the leading order effective constant ρ_s: the spin stiffness.

We have explored the effect of the spin-wave interaction on various thermodynamic quantities as a function of external magnetic and staggered fields. As it turns out, the interaction in the pressure is small and may be attractive or repulsive. If temperature is raised from $T = 0$ to a nonzero value T – while keeping the staggered and magnetic field strengths fixed – the order parameter and magnetization may decrease or increase on account of the spin-wave interaction. The latter observation is rather counterintuitive.

A Auxiliary Expressions for Two-Loop Free Energy Density

In this appendix, we collect the necessary definitions to make the expression (2.8) for the renormalized two-loop free energy density self-contained. The zero-temperature part of the free energy takes the explicit form

$$z^{[0]} = -M_s H_s - \frac{\rho_s}{2} H^2$$

$$
\begin{aligned}
&+\frac{H^4}{64\pi^2}\left(-\frac{1}{2}+\ln\frac{M_I^2}{\mu^2}+\frac{\bar{e}_1}{3}-\frac{4\bar{e}_2}{3}\right)+\frac{H^2M_sH_s}{64\pi^2\rho_s}\left(-1+2\ln\frac{M_I^2}{\mu^2}-2\bar{k}_1\right)\\
&+\frac{M_s^2H_s^2}{64\pi^2\rho_s^2}\left(-1+\ln\frac{M_I^2}{\mu^2}+\ln\frac{M_{II}^2}{\mu^2}-2\bar{k}_2-2\bar{k}_3\right)\\
&+\frac{1}{1024\pi^4}\left(c_{6,0}\frac{H^6}{\rho_s}+c_{4,1}\frac{H^4M_sH_s}{\rho_s^2}+c_{2,2}\frac{H^2M_s^2H_s^2}{\rho_s^3}+c_{0,3}\frac{M_s^3H_s^3}{\rho_s^4}\right)\\
&-\frac{H^2}{128\pi^4\rho_s}M_IM_{II}^3\int_0^\infty \mathrm{d}x\,R(x,M_{II}/M_I)\,.
\end{aligned}
\tag{A.1}
$$

The first two lines give the zero- and one-loop contributions to the free energy, respectively. The rest represents the two-loop free energy, evaluated first in Ref. [34]. The numerical coefficients $c_{i,3-\frac{i}{2}}$ appearing therein are defined by

$$
\begin{aligned}
c_{6,0} &= \frac{1}{4}-\frac{\gamma_\mathrm{E}}{6}+\frac{1}{6}\ln 4\pi-\frac{2}{3}\ln\frac{M_I^2}{\mu^2}-\ln^2\frac{M_I^2}{\mu^2}+\bar{e}_2\left(\frac{1}{3}+2\ln\frac{M_I^2}{\mu^2}\right)\,,\\
c_{4,1} &= \frac{11}{4}+\frac{13\gamma_\mathrm{E}}{6}-5\gamma_\mathrm{E}^2-\frac{\pi^2}{6}+\frac{11}{6}\ln 4\pi-4\ln 2+8\gamma_\mathrm{E}\ln 2-4\ln^2 2\\
&\quad-\frac{13}{3}\ln\frac{M_I^2}{\mu^2}-\frac{3}{2}\ln^2\frac{M_I^2}{\mu^2}+\left(\frac{2\bar{e}_1}{3}+\bar{k}_1\right)\ln\frac{M_I^2}{\mu^2}+\frac{2\bar{e}_2}{3}\left(1+2\ln\frac{M_I^2}{\mu^2}\right)\,,\\
c_{2,2} &= \frac{23}{8}+\frac{49\gamma_\mathrm{E}}{12}-\frac{15\gamma_\mathrm{E}^2}{2}-\frac{\pi^2}{4}+\frac{23}{12}\ln 4\pi-6\ln 2+12\gamma_\mathrm{E}\ln 2-6\ln^2 2\\
&\quad-\frac{14}{3}\ln\frac{M_I^2}{\mu^2}+2(\gamma_\mathrm{E}-\ln 2)\ln\frac{M_I^2}{M_{II}^2}-\frac{3}{2}\ln^2\frac{M_I^2}{\mu^2}+2\ln\frac{M_I^2}{\mu^2}\ln\frac{M_{II}^2}{\mu^2}\\
&\quad+\bar{e}_1\left(-\frac{1}{6}+\frac{2}{3}\ln\frac{M_I^2}{\mu^2}+\ln\frac{M_{II}^2}{\mu^2}\right)+\bar{e}_2\left(1-\frac{2}{3}\ln\frac{M_I^2}{\mu^2}-4\ln\frac{M_{II}^2}{\mu^2}\right)\\
&\quad-\bar{k}_1\ln\frac{M_I^2}{M_{II}^2}+2\bar{k}_2\ln\frac{M_I^2}{\mu^2}\,,\\
c_{0,3} &= -\frac{1}{2}\ln^2\frac{M_I^2}{M_{II}^2}-2(\bar{k}_1-\bar{k}_2)\left(\ln\frac{M_I^2}{\mu^2}+\ln\frac{M_{II}^2}{\mu^2}\right)\,.
\end{aligned}
\tag{A.2}
$$

Finally, the last line of Eq. (A.1) is the only contribution that cannot be evaluated in a closed form, and is rather given by a simple one-dimensional integral, defined in terms of a residuum $R(x,\alpha)$ in an asymptotic expansion of a product of modified Bessel functions of the second kind,

$$
\begin{aligned}
[K_1(x)]^2K_1(\alpha x) &= \frac{1}{\alpha}\frac{1}{x^3}+\left(\frac{\alpha}{2}+\frac{1}{\alpha}\right)\frac{\ln x}{x}e^{-x^2}\\
&\quad+\left[\left(-\frac{1}{4}+\frac{\gamma_\mathrm{E}}{2}\right)\alpha+\left(-\frac{1}{2}+\gamma_\mathrm{E}-\ln 2\right)\frac{1}{\alpha}+\frac{\alpha}{2}\ln\frac{\alpha}{2}\right]\frac{1}{e^x-1}\\
&\quad+R(x,\alpha)\,.
\end{aligned}
\tag{A.3}
$$

In order to complete the definition of the thermal part of the free energy density (2.8), we need to specify the dimensionless function $\hat{s}$. The dimension*ful* combi-

nation $\frac{2}{\rho_s}\,\hat{s}\,T^6$, appearing in Eq. (2.8), is defined by a subtracted integral,

$$s = \frac{2H^2}{\rho_s}\left(\int_{\mathcal{T}} \mathrm{d}^4x\, T + \int_{\mathcal{T}\setminus\mathcal{S}} \mathrm{d}^4x\, U + \int_{\mathcal{S}} \mathrm{d}^4x\, V - \int_{\mathbb{R}^D\setminus\mathcal{S}} \mathrm{d}^4x\, W\right), \tag{A.4}$$

where the individual contributions read [34]

$$\begin{aligned}
T &= \overline{G}^I\partial_0\overline{G}^I\partial_0\overline{G}^{II} + \Delta^I\partial_0\overline{G}^I\partial_0\overline{G}^{II} + \overline{G}^I\partial_0\Delta^I\partial_0\overline{G}^{II} + \overline{G}^I\partial_0\overline{G}^I\partial_0\Delta^{II}\,,\\
U &= \Delta^I\partial_0\overline{G}^I\partial_0\Delta^{II} + \Delta^I\partial_0\Delta^I\partial_0\overline{G}^{II} + \overline{G}^I\partial_0\Delta^I\partial_0\Delta^{II} + \Delta^I\partial_0\Delta^I\partial_0\Delta^{II}\,,\\
V &= \Delta^I\left[\partial_0\overline{G}^I - x_0\left(\frac{3}{2}g_0^I + M_I^2 g_1^I\right)\right]\partial_0\Delta^{II} + \Delta^I\partial_0\Delta^I\left[\partial_0\overline{G}^{II} - x_0\left(\frac{3}{2}g_0^{II} + M_{II}^2 g_1^{II}\right)\right]\\
&\quad + \left[\overline{G}^I - g_1^I + \frac{1}{4}(\boldsymbol{x}^2 - 3x_0^2)g_0^I - \frac{1}{2}x_0^2 M_I^2 g_1^I\right]\partial_0\Delta^I\partial_0\Delta^{II}\,,\\
W &= \Delta^I x_0\left(\frac{3}{2}g_0^I + M_I^2 g_1^I\right)\partial_0\Delta^{II} + \Delta^I\partial_0\Delta^I x_0\left(\frac{3}{2}g_0^{II} + M_{II}^2 g_1^{II}\right)\\
&\quad + \left[g_1^I - \frac{1}{4}(\boldsymbol{x}^2 - 3x_0^2)g_0^I + \frac{1}{2}x_0^2 M_I^2 g_1^I\right]\partial_0\Delta^I\partial_0\Delta^{II} + \Delta^I\partial_0\Delta^I\partial_0\Delta^{II}\,.
\end{aligned} \tag{A.5}$$

Here $\Delta(x)$ and $\overline{G}(x)$ are the zero-temperature and finite-temperature parts of the thermal propagator of a free massive relativistic particle,

$$G(x) = \Delta(x) + \overline{G}(x). \tag{A.6}$$

Finally, the symbol $\mathcal{T}$ in Eq. (A.4) denotes the domain of integration in thermal field theory in $d = D-1$ spatial dimensions, that is the torus $S^1\times\mathbb{R}^d$. The small sphere $\mathcal{S}$ near the origin is cut out in order to regulate the ultraviolet divergences, and the final result of integration is independent of the size of the sphere.

B Alternative Evaluation of Magnon Self-Energy

In this appendix we sketch an alternative evaluation of the self-energy for the two types of magnons at the one-loop level. In contrast to the calculation carried out in the main text, we will show how to find the self-energies using coordinate-space techniques. The relevant Feynman graphs for the two-point function are depicted in Fig. 2. The leading contribution to the two-point function $\tau_{I,II}(x-y)$ is given by the dimensionally regularized propagator $\Delta_{I,II}(x-y)$,

$$\tau^{4a}_{I,II}(x-y) = \Delta_{I,II}(x-y) = \int\frac{\mathrm{d}^dk}{(2\pi)^d}\,\frac{e^{ik(x-y)}}{k_0^2+\vec{k}^2+M_{I,II}^2}\,, \tag{B.1}$$

respectively for the magnon with mass M_I or M_{II}. The individual pieces that yield corrections to $\Delta_{I,II}(x-y)$ are

$$\tau^{6a}_I(x-y) = \left[-\left(\frac{M_sH_s}{4\rho_s^3} + \frac{H^2}{\rho_s^2}\right)\Delta_I(0) + \frac{M_sH_s}{4\rho_s^3}\Delta_{II}(0)\right]\int\frac{\mathrm{d}^dk}{(2\pi)^d}\,\frac{e^{ik(x-y)}}{\left(k_0^2+\vec{k}^2+M_I^2\right)^2}\,,$$

$$
\begin{aligned}
\tau_{II}^{6a}(x-y) = &\left[\frac{M_s H_s}{4\rho_s^3}\Delta_I(0) - \frac{M_s H_s}{4\rho_s^3}\Delta_{II}(0)\right] \int\frac{\mathrm{d}^d k}{(2\pi)^d}\, \frac{e^{ik(x-y)}}{\left(k_0^2+\vec{k}^2+M_{II}^2\right)^2}\,, \\
\tau_{I}^{6b}(x-y) = &\left[(k_2-k_1)\frac{M_s^2 H_s^2}{\rho_s^4} + (\tfrac{1}{2}k_1 - 2e_1)\frac{M_s H_s H^2}{\rho_s^3} + \frac{2e_2 H^4}{\rho_s^2}\right] \int\frac{\mathrm{d}^d k}{(2\pi)^d} \frac{e^{ik(x-y)}}{\left(k_0^2+\vec{k}^2+M_{I}^2\right)^2}\,, \\
&+ \frac{2e_2 H^2}{\rho_s^2} \int\frac{\mathrm{d}^d k}{(2\pi)^d} \frac{e^{ik(x-y)}}{\left(k_0^2+\vec{k}^2+M_{I}^2\right)^2}\, k_0^2\,, \\
\tau_{II}^{6b}(x-y) = &\left[(k_2-k_1)\frac{M_s^2 H_s^2}{\rho_s^4} + (\tfrac{1}{2}k_1 - 2e_1 - 2e_2)\frac{M_s H_s H^2}{\rho_s^3}\right] \int\frac{\mathrm{d}^d k}{(2\pi)^d} \frac{e^{ik(x-y)}}{\left(k_0^2+\vec{k}^2+M_{II}^2\right)^2}\,, \\
&+ \frac{4(e_1+e_2) H^2}{\rho_s^2} \int\frac{\mathrm{d}^d k}{(2\pi)^d} \frac{e^{ik(x-y)}}{\left(k_0^2+\vec{k}^2+M_{II}^2\right)^2}\, k_0^2\,, \\
\tau_{I,II}^{6c}(x-y) = &\, 0\,, \qquad\qquad \text{(B.2)} \\
\tau_{I}^{6d}(x-y) = &\frac{2H^2}{\rho_s^2} \int\frac{\mathrm{d}^d k}{(2\pi)^d}\frac{\mathrm{d}^d q}{(2\pi)^d} \frac{e^{ik(x-y)}}{\left(k_0^2+\vec{k}^2+M_{I}^2\right)^2} \frac{1}{q_0^2+\vec{q}^2+M_I^2} \frac{(k_0-q_0)^2}{(k_0-q_0)^2+(\vec{k}-\vec{q})^2+M_{II}^2}\,, \\
\tau_{II}^{6d}(x-y) = &\frac{2H^2}{\rho_s^2} \int\frac{\mathrm{d}^d k}{(2\pi)^d}\frac{\mathrm{d}^d q}{(2\pi)^d} \frac{e^{ik(x-y)}}{\left(k_0^2+\vec{k}^2+M_{II}^2\right)^2} \frac{1}{q_0^2+\vec{q}^2+M_I^2} \frac{k_0(k_0-q_0)}{(k_0-q_0)^2+(\vec{k}-\vec{q})^2+M_{I}^2}\,.
\end{aligned}
$$

With the relations

$$
\begin{aligned}
\int\frac{\mathrm{d}^d q}{(2\pi)^d} \frac{1}{\left[(p-q)^2+m_1^2\right]\left(q^2+m_2^2\right)} &= \frac{\Gamma(2-d/2)}{(4\pi)^{d/2}} \int_0^1 \mathrm{d}\alpha\; I^{d/2-2}\,, \\
\int\frac{\mathrm{d}^d q}{(2\pi)^d} \frac{q_0}{\left[(p-q)^2+m_1^2\right]\left(q^2+m_2^2\right)} &= p_0\frac{\Gamma(2-d/2)}{(4\pi)^{d/2}} \int_0^1 \mathrm{d}\alpha\; I^{d/2-2}\alpha\,, \\
\int\frac{\mathrm{d}^d q}{(2\pi)^d} \frac{q_0^2}{\left[(p-q)^2+m_1^2\right]\left(q^2+m_2^2\right)} &= \frac{\Gamma(1-d/2)}{2(4\pi)^{d/2}} \int_0^1 \mathrm{d}\alpha\; I^{d/2-1} \\
&\quad + p_0^2\, \frac{\Gamma(2-d/2)}{(4\pi)^{d/2}} \int_0^1 \mathrm{d}\alpha\; I^{d/2-2}\alpha^2
\end{aligned}
\qquad \text{(B.3)}
$$

and

$$
I = \alpha(1-\alpha)p^2 + \alpha m_1^2 + (1-\alpha)m_2^2\,, \qquad \text{(B.4)}
$$

the integration over momentum q in $\tau_{I,II}^{6d}(x-y)$ is straightforward in dimensional regularization. The various contributions can be merged into the physical two-point function $\tau_{I,II}(x-y)$ by expanding its denominator as

$$
\begin{aligned}
\tau_{I,II}(x-y) &= \int\frac{\mathrm{d}^d k}{(2\pi)^d}\, \frac{e^{ik(x-y)}}{k_0^2+\vec{k}^2+M_{I,II}^2+X_{I,II}} \qquad \text{(B.5)} \\
&= \int\frac{\mathrm{d}^d k}{(2\pi)^d}\, \frac{e^{ik(x-y)}}{k_0^2+\vec{k}^2+M_{I,II}^2} \left[1 - \frac{X_{I,II}}{k_0^2+\vec{k}^2+M_{I,II}^2} + \mathcal{O}(X^2/\mathcal{D}^2)\right]\,,
\end{aligned}
$$

where

$$\mathcal{D} = k_0^2 + \vec{k}^2 + M_{I,II}^2 \tag{B.6}$$

is the inverse free propagator in momentum space. The quantity $X_{I,II}$ corresponds to higher-order corrections of the dispersion relation. Up to next-to-leading order in the momentum expansion, $X_{I,II}$ is fixed by the expressions (B.2).

Taking the physical limit $d \to 4$, ultraviolet singularities emerge as poles in the Γ-function contained in $\tau_{I,II}^{6d}(x-y)$ [see Eq. (B.3)], as well as in $\tau_{I,II}^{6a}(x-y)$ [on account of $\Delta_I(0)$ and $\Delta_{II}(0)$]. Likewise, the NLO effective constants e_1, e_2, k_1, k_2 showing up in $\tau_{I,II}^{6b}(x-y)$, become divergent in the limit $d \to 4$. We will, however, not delve into details here, because the renormalization procedure concerning the two-point function is standard and completely analogous to the procedure regarding the free energy density, outlined in much detail in Ref. [34]. We just spell out the essential result, namely, that the various subdivergences contained in the above representations for the two-point function cancel, and that the resulting dispersion relations for the two magnons at one-loop order are free of singularities. They amount to

$$\begin{aligned} \omega_I^2 &= \vec{k}^2 + M_I^2 + \alpha_I k_0^2 + \beta_I \,, \\ \omega_{II}^2 &= \vec{k}^2 + M_{II}^2 + \alpha_{II} k_0^2 + \beta_{II} \,, \end{aligned} \tag{B.7}$$

with coefficients

$$\begin{aligned}
\alpha_I &= \frac{1}{72\pi^2\rho_s M_I^4}\Big((6\overline{e}_2-2)H^6 + (12\overline{e}_2-13)H^4M_{II}^2 + (6\overline{e}_2-5)H^2M_{II}^4\Big) \\
&\quad + \frac{1}{12\pi^2\rho_s M_I^6}\, H^4M_{II}^3\sqrt{4H^2+3M_{II}^2}\Big(\arctan\frac{M_{II}}{\sqrt{4H^2+3M_{II}^2}} + \arctan\frac{2H^2+M_{II}}{M_{II}\sqrt{4H^2+3M_{II}^2}}\Big) \\
&\quad + \frac{H^2}{24\pi^2\rho_s M_I^6}\Big((3H^2M_{II}^4+2M_{II}^6)\log\frac{M_{II}^2}{\mu^2} - (2H^6+6H^4M_{II}^2+9H^2M_{II}^4+4M_{II}^6)\log\frac{M_I^2}{\mu^2}\Big)\,, \\
\beta_I &= \frac{1}{288\pi^2\rho_s M_I^2}\Big(8(3\overline{e}_2-1)H^6 + (6\overline{e}_1+24\overline{e}_2+9\overline{k}_1-52)H^4M_{II}^2 \\
&\quad + (6\overline{e}_2-9\overline{k}_1+18\overline{k}_2-38)H^2M_{II}^4 + 18(\overline{k}_2-\overline{k}_1)M_{II}^6\Big) \\
&\quad + \frac{1}{48\pi^2\rho_s M_I^4}\, H^2M_{II}^3(4H^2+3M_{II}^2)^{3/2}\Big(\arctan\frac{M_{II}}{\sqrt{4H^2+3M_{II}^2}} + \arctan\frac{2H^2+M_{II}}{M_{II}\sqrt{4H^2+3M_{II}^2}}\Big) \\
&\quad + \frac{1}{96\pi^2\rho_s M_I^4}\Big((9H^4M_{II}^4+11H^2M_{II}^6+3M_{II}^8)\log\frac{M_{II}^2}{\mu^2} \\
&\quad - (8H^8+21H^6M_{II}^2+27H^4M_{II}^4+16H^2M_{II}^6+3M_{II}^8)\log\frac{M_I^2}{\mu^2}\Big)\,, \\
\alpha_{II} &= -\frac{1}{24\pi^2\rho_s}\,(\overline{e}_1-4\overline{e}_2-3)H^2 \\
&\quad - \frac{1}{4\pi^2\rho_s M_{II}}H^2\sqrt{4H^2+3M_{II}^2}\arctan\frac{M_{II}}{\sqrt{4H^2+3M_{II}^2}}
\end{aligned}$$

$$
\begin{aligned}
& -\frac{1}{8\pi^2\rho_s}\, H^2 \log\frac{M_I^2}{\mu^2}\,, \\
\beta_{II} \;=\; & \frac{1}{96\pi^2\rho_s}\,\Big((2\overline{e}_1-8\overline{e}_2+3\overline{k}_1)H^2M_{II}^2+6(\overline{k}_2-\overline{k}_1)M_{II}^4\Big) \\
& +\frac{1}{32\pi^2\rho_s}\,\Big(-M_{II}^4\log\frac{M_{II}^2}{\mu^2}+M_{II}^2M_I^2\log\frac{M_I^2}{\mu^2}\Big)\,.
\end{aligned}
\tag{B.8}
$$

These provide an explicit realization of the NLO dispersion relations (3.2). It should be stressed that the μ-dependence of the renormalized NLO effective constants $\overline{e}_1$, $\overline{e}_2$, $\overline{k}_1$, $\overline{k}_2$ – see Eq. (2.12) – is canceled by the μ-dependent logarithms in Eq. (B.8): the dispersion relations – much like the free energy density – do not depend on the renormalization scale μ. These cancellations provide a nontrivial check of the calculation.

We can now isolate the piece in the free energy density that refers to the spin-wave interaction. On the one hand, we have calculated the purely noninteracting part z_{free} via Eq. (3.3) using the dressed magnons. On the other hand, in Sec. 2, we have provided the full two-loop representation z for the free energy density, Eq. (2.8), that includes both the interacting and noninteracting part. The purely interaction part is given by the difference

$$
z_{int} = z - z_{free}\,,
\tag{B.9}
$$

that amounts to

$$
\begin{aligned}
z_{int} = \; & -\frac{4H^2+M_{II}^2}{8\rho_s}\big(g_1^I\big)^2+\frac{M_{II}^2}{4\rho_s}g_1^Ig_1^{II}-\frac{M_{II}^2}{8\rho_s}\big(g_1^{II}\big)^2+\frac{2}{\rho_s}\,\hat{s}\,T^6 \\
& +\frac{1}{32\pi^2\rho_s}(\mathcal{C}_0^Ig_0^I+\mathcal{C}_0^{II}g_0^{II}+\mathcal{C}_1^Ig_1^I+\mathcal{C}_1^{II}g_1^{II})+z^{[0]}-z_{free}^{[0]}\,.
\end{aligned}
\tag{B.10}
$$

The coefficients accompanying the kinematical functions read

$$
\begin{aligned}
\mathcal{C}_0^I = \; & \frac{H^8-3H_{II}^2M_{II}^6-2M_{II}^8}{H^2(H^2+M_{II}^2)^2}+\frac{2H^4M_{II}^3\sqrt{4H^2+3M_{II}^2}}{(H^2+M_{II}^2)^3}\arctan\frac{M_{II}}{\sqrt{4H^2+3M_{II}^2}} \\
& +\frac{2H^4M_{II}^3\sqrt{4H^2+3M_{II}^2}}{(H^2+M_{II}^2)^3}\arctan\frac{2H^2+M_{II}^2}{M_{II}\sqrt{4H^2+3M_{II}^2}} \\
& +\frac{M_{II}^4(-3H^8+6H^4M_{II}^4+6H^2M_{II}^6+2M_{II}^8)}{H^2(H^2+M_{II}^2)^3}\log\frac{M_I^2}{M_{II}^2}\,, \\
\mathcal{C}_0^{II} = \; & 6H^2-\frac{6H^2\sqrt{4H^2+3M_{II}^2}}{M_{II}}\arctan\frac{M_{II}}{\sqrt{4H^2+3M_{II}^2}}\,, \\
\mathcal{C}_1^I = \; & \frac{2H^8+6H^2M_{II}^6-7H^4M_{II}^4-24H^2M_{II}^6-12M_{II}^8}{6H^2(H^2+M_{II}^2)} \\
& +\frac{H^2M_{II}^5\sqrt{4H^2+3M_{II}^2}}{(H^2+M_{II}^2)^2}\arctan\frac{M_{II}}{\sqrt{4H^2+3M_{II}^2}} \\
& +\frac{2H^4M_{II}^3\sqrt{4H^2+3M_{II}^2}}{(H^2+M_{II}^2)^2}\arctan\frac{H^2+M_{II}^5}{M_{II}\sqrt{4H^2+3M_{II}^2}}
\end{aligned}
\tag{B.11}
$$

$$+\frac{M_{II}^4(2H^8+13H^6M_{II}^2+20H^4M_{II}^4+14H^2M_{II}^6+4M_{II}^8)}{2H^4(H^2+M_{II}^2)^2}\log\frac{M_I^2}{M_{II}^2}\,,$$

$$\mathcal{C}_1^{II}=4H^2M_{II}^2-4\sqrt{4H^2+3M_{II}^2}\arctan\frac{M_{II}}{\sqrt{4H^2+3M_{II}^2}}\,.$$

This is an alternative expression for the result given in Eq. (3.14) of the main text. Note that the next-to-leading-order effective constants and the μ-dependent logarithms have been absorbed into the noninteracting magnon free energy density by redefining the dispersion relations as described above. In particular, the absence of the (a priori) unknown NLO effective constants $\overline{e}_1, \overline{e}_2, \overline{k}_1, \overline{k}_2$ in Eq. (B.11) means that our result regarding the impact of the spin-wave interaction is parameter-free.

References

[1] T. Oguchi, Phys. Rev. **117**, 117 (1960).

[2] F. Keffer and R. Loudon, J. Appl. Phys. (Suppl.) **32**, 2 (1961).

[3] T. Oguchi and A. Honma, J. Appl. Phys. **34**, 1153 (1963).

[4] A. B. Harris, J. Appl. Phys. **35**, 798 (1964).

[5] K. H. Lee and S. H. Liu, Phys. Rev. **159**, 390 (1967).

[6] O. Nagai, Phys. Rev. **180**, 557 (1969).

[7] M. G. Cottam and R. B. Stinchcombe, J. Phys. C: Solid St. Phys. **3**, 2326 (1970).

[8] A. B. Harris, D. Kumar, B. I. Halperin, and P. C. Hohenberg, Phys. Rev. B **3**, 961 (1971).

[9] B.-G. Liu, Phys. Lett. A **259**, 308 (1999).

[10] N. Hasselmann and P. Kopietz, Europhys. Lett. **74**, 1067 (2006).

[11] M. I. Kaganov and V. M. Tsukernik, Sov. Phys. JETP **34**, 1107 (1958).

[12] A. I. Akhiezer, V. G. Baryakhtar, and M. I. Kaganov, Sov. Phys. Usp. **3**, 567 (1961).

[13] H. Falk, Phys. Rev. **133**, A1382 (1964).

[14] E. M. Pikalev, M. A. Savchenko, and J. Solyom, Sov. Phys. JETP **28**, 734 (1969).

[15] J. Solyom, Sov. Phys. JETP **28**, 1251 (1969).

[16] M. G. Cottam and R. B. Stinchcombe, J. Phys. C: Solid St. Phys. **3**, 2283 (1970).

[17] D. S. Fisher, Phys. Rev. B **39**, 11783 (1989).

[18] C. Millán and D. Gottlieb, Phys. Rev. B **50**, 242 (1994).

[19] E. B. Filho and J. R. de Sousa, Phys. Lett. A **323**, 9 (2004).

[20] A. Kreisel, F. Sauli, N. Hasselmann, and P. Kopietz, Phys. Rev. B **78**, 035127 (2008).

[21] M. A. Neto, J. R. Viana, and J. R. de Sousa, J. Magn. Mag. Mat. **324**, 2405 (2012).

[22] J. Gasser and H. Leutwyler, Ann. Phys. (N.Y.) **158**, 142 (1984).

[23] J. Gasser and H. Leutwyler, Nucl. Phys. B **250**, 465 (1985).

[24] H. Leutwyler, Phys. Rev. D **49**, 3033 (1994).

[25] J. O. Andersen, T. Brauner, C. P. Hofmann, and A. Vuorinen, J. High Energy Phys. 08 (2014) 088.

[26] P. Hasenfratz and H. Leutwyler, Nucl. Phys. B **343**, 241 (1990).

[27] C. P. Hofmann, Phys. Rev. B **60**, 388 (1999).

[28] C. P. Hofmann, Phys. Rev. B **60**, 406 (1999).

[29] J. M. Román and J. Soto, Int. J. Mod. Phys. B **13**, 755 (1999).

[30] J. M. Román and J. Soto, Ann. Phys. **273**, 37 (1999).

[31] J. M. Román and J. Soto, Phys. Rev. B **62**, 3300 (2000).

[32] C. P. Hofmann, Nucl. Phys. B **916**, 254 (2017).

[33] C. P. Hofmann, Phys. Rev. B **95**, 134402 (2017).

[34] T. Brauner and C. P. Hofmann, Ann. Phys. **386**, 178 (2017).

[35] F. Bloch, Z. Phys. **61**, 206 (1930).

[36] F. J. Dyson, Phys. Rev. **102**, 1217 (1956).

[37] F. J. Dyson, Phys. Rev. **102**, 1230 (1956).

[38] C. P. Hofmann, Phys. Rev. B **84**, 064414 (2011).

[39] C. P. Hofmann, Physica B **510**, 117 (2017).

[40] W. Nolting, *Quantentheorie des Magnetismus* (Teubner, Stuttgart, 1986), Band 2.

[41] V. Jaccarino, in: Magnetism, Vol. IIA, G. T. Rado and H. Suhl eds. (Academic, New York, 1965), p. 331.

[42] L. J. de Jongh and A. R. Miedema, Adv. Phys. **23**, 1 (1974), and references therein.

[43] A. Tucciarone, H. Y. Lau, L. M. Corliss, A. Delapalme, and J. M. Hastings, Phys. Rev. B **4**, 3206 (1971).

[44] A. Tucciarone, J. M. Hastings, and L. M. Corliss, Phys. Rev. B **8**, 1103 (1973).

[45] F. Keffer, *Spin Waves*, in *Encyclopedia of Physics – Ferromagnetism*, edited by S. Flügge and H. P. J. Wijn (Springer, Berlin, 1966), Vol.18-2, p.1.